Journal of
Clinical Pathology

Denosumab treated giant cell tumor of bone: A morphological, immunohistochemical and molecular analysis of a series.

Journal:	*Journal of Clinical Pathology*
Manuscript ID:	jclinpath-2015-203248.R1
Article Type:	Original Article
Date Submitted by the Author:	n/a
Complete List of Authors:	Girolami, Ilaria; University of Florence, Department of Surgery and Translational Medicine Mancini, Irene; University of Florence, Department of Biomedical, Experimental and Clinical Sciences Simoni, Antonella; University of Florence, Department of Surgery and Translational Medicine Baldi, Giacomo; Hospital of Prato, "Sandro Pitigliani" Medical Oncology Department Simi, Lisa; University of Florence, Department of Biomedical, Experimental and Clinical Sciences Campanacci, Domenico; Azienda Ospedaliero-Universitaria Careggi, Department of Orthopedic Oncology Beltrami, Giovanni; Azienda Ospedaliero-Universitaria Careggi, Department of Orthopedic Oncology Scoccianti, Guido; Azienda Ospedaliero-Universitaria Careggi, Department of Orthopedic Oncology D'Arienzo, Antonio; Azienda Ospedaliero-Universitaria Careggi, Department of Orthopedic Oncology Capanna, Rodolfo; Azienda Ospedaliero-Universitaria Careggi, Department of Orthopedic Oncology Franchi, Alessandro; University of Florence, Department of Surgery and Translational Medicine
Keywords:	BONE TUMOURS, IMMUNOCYTOCHEMISTRY, CANCER GENETICS
Specialty:	Histopathology

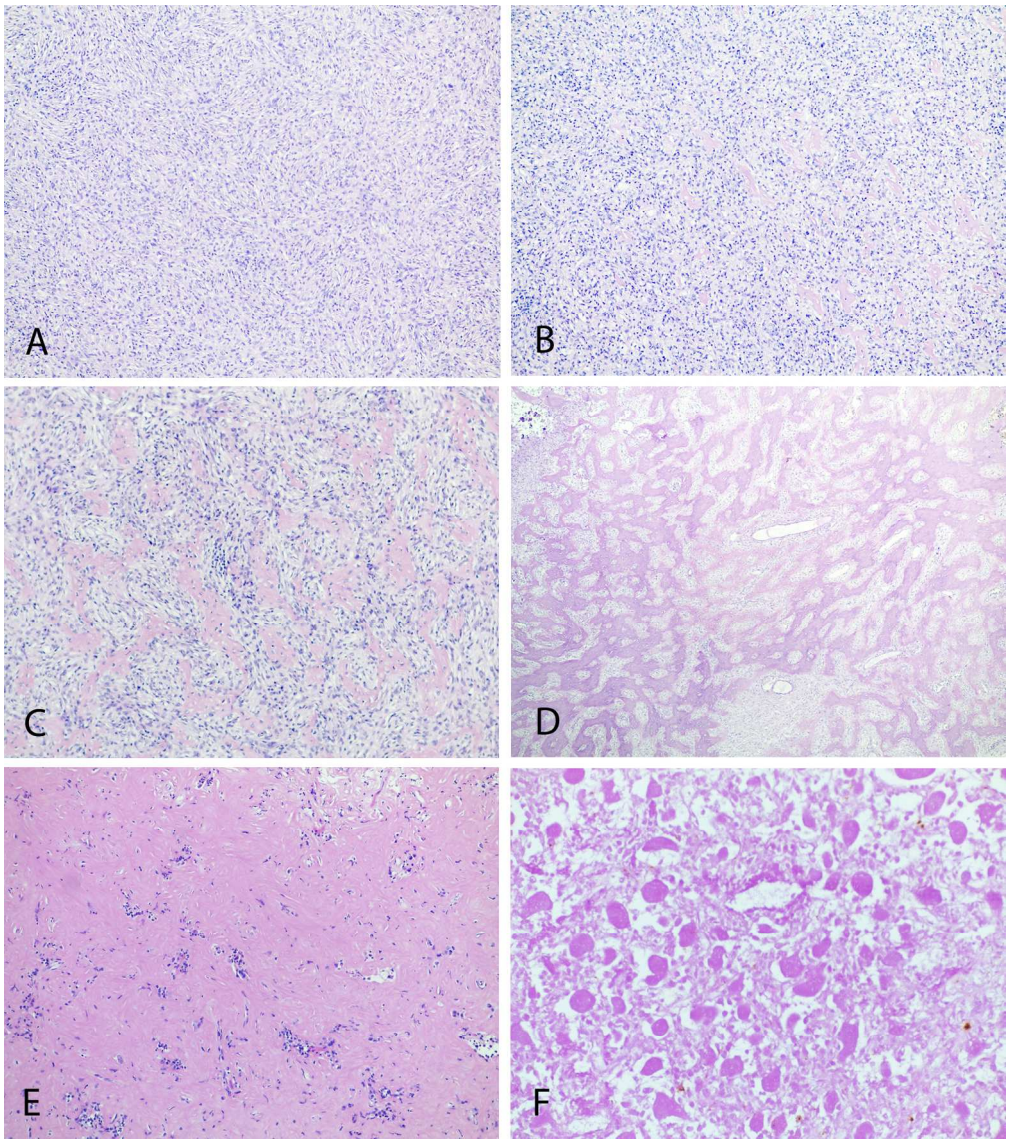

161x183mm (300 x 300 DPI)

Denosumab treated giant cell tumor of bone: A morphological, immunohistochemical and molecular analysis of a series.

Ilaria Girolami,[1]* Irene Mancini,[2]* Antonella Simoni,[1] Giacomo Giulio Baldi,[3] Lisa Simi,[2] Domenico Campanacci,[4] Giovanni Beltrami,[4] Guido Scoccianti,[4] Antonio D'Arienzo,[4] Rodolfo Capanna,[4] and Alessandro Franchi[1]

[1]Department of Surgery and Translational Medicine, University of Florence, Italy
[2]Department of Clinical and Experimental Biomedical Sciences, University of Florence, Italy
[3]"Sandro Pitigliani" Medical Oncology Department, Hospital of Prato, Italy
[4]Department of Orthopaedic Oncology, Azienda Ospedaliero-Universitaria Careggi, Florence, Italy

*These Authors contributed equally to the paper

Key words: giant cell tumor of bone, denosumab, RANK, RANKL, SATB2, RUNX2, angiogenesis, immunohistochemistry, histone 3.3 mutation analysis

Corresponding Author:

Alessandro Franchi, MD
Division of Anatomic Pathology
Department of Surgery and Translational Medicine
University of Florence
Largo Brambilla 3
50134, Florence
Italy
Phone: +39 055 4478102
Fax: + 39 055 4379868
E-mail: franchi@unifi.it

Abstract

Background. Denosumab, a fully human monoclonal antibody directed against RANKL, has recently been introduced in the treatment strategy of giant cell tumor of bone (GCTB). Aim of this study was to investigate the phenotypic modifications induced by Denosumab treatment in a series of 15 GCTB.

Methods. The tumors were characterized for histone 3.3 mutations, and studied immunohistochemically for the modifications of RANKL, RANK, SATB2 and RUNX2 expression, as well as of tumor proliferative activity and angiogenesis.

Results. Nine of 11 tumors investigated presented a histone 3.3 mutation in *H3F3A*, and 2 of these for which the analysis was carried out in pre- and post-treatment specimens showed the same mutation in both. Denosumab induced the disappearance of osteoclast-like giant cells, leaving residual spindle neoplastic cells arranged in a storiform pattern, with deposition of trabecular collagen matrix and osteoid, which tended to maturation in the peripheral portions of the lesion. RANK and RANKL expression was variable, with no significant variation after treatment. Moreover, we did not observe any significant modification of the expression of the osteoblastic markers SATB2 and RUNX2. Denosumab treatment determined a significant reduction of the proliferative index and of tumor angiogenesis (p=0.001, Wilcoxon Ranks Sum Test).

Conclusions. These results indicate that Denosumab induces a partial maturation towards the osteoblastic phenotype of the neoplastic cells of GCTB, with production of fibrous and osteoid matrix, but with minor immunophenotypic changes. Finally, we first report an antiangiogenic activity of Denosumab in GCTB, possibly mediated by a RANKL-dependent pathway.

Introduction

Giant cell tumor of bone (GCTB) is a rare locally aggressive tumor, which most often affects young adults with predilection for the epiphyses of long bones [1]. Histologically, the tumor consists of a proliferation of mononuclear cells, accompanied by a population of non-neoplastic osteoclast-like giant cells and mononuclear osteoclast precursors. Currently, it is thought that proliferating neoplastic cells produce a number of cytokines and mediators, including the receptor activator of nuclear factor kappa-B-ligand (RANK-RANKL) system, that recruit osteoclast precursors and induce their maturation into multinucleated osteoclast. These cells ultimately determine bone destruction and allow the growth of the tumor. Recently, a putative driver mutation in the *H3F3A* gene of histone 3.3 has been identified as a specific genetic change of GCTB [2].

The standard management of GCTB is based on surgery with several local adjuvant treatments like metacrylate cement, phenol or criotherapy to reduce the risk of recurrence, while bisphosphonates are used in some cases to decrease bone resorption and for pain relief in inoperable tumors or metastatic disease [3]. In the last five years the use of Denosumab, a fully human monoclonal antibody already licensed for postmenopausal osteoporosis and prevention of skeletal related events in bone metastases from solid tumors, has been introduced in the treatment strategy of GCTB [4]. This antibody specifically binds to RANKL, preventing its interaction with RANK and thus the formation of osteoclastic giant cells and the consequent excessive bone resorption. Denosumab has shown to be a turning point in the management of GCTB, allowing treatment of patients that cannot undergo surgery due to excessive morbidity for the anatomical location of the lesion and allowing a less morbid surgery after reduction of the osteolytic area, with general beneficial effects on patients' symptoms [3, 4].

In this study we examined the histological and immunophenotypic features of a series of GCTB, characterized for histone 3.3 mutations, before and after Denosumab

administration, comparing baseline and resection specimens. In particular, we investigated the modifications in the expression of RANKL and RANK, and of the osteoblastic markers SATB2 and RUNX2. Moreover, we examined the effects of the treatment on tumor proliferative activity and on the angiogenesis through the determination of microvascular density.

Patients and methods

Patients

Clinical data of the 15 patients who received Denosumab treatment pre-operatively are summarized in Table 1. All but one patients were affected by primary skeletal lesions. The only exception was a patient who presented a local soft tissue recurrence of a GCTB of the distal femur which had been treated 16 months before with curettage.

After screening for contraindications and informed consent acquisition, patients were treated pre-operatively with Denosumab 120 mg SC (day 1, 8, 15, 28 and every 4 weeks thereafter) for at least three months and then post-operatively every 4 weeks for 6 months. Timing of surgery was based on clinical and radiological findings, the median time on pre-operative Denosumab was 5.7 months (range 3-6). All patients underwent surgery, which consisted of curettage with local adjuvant treatments in nine cases and tumor resection in six cases. At a median follow-up of 13 months, three patients developed a local recurrence and are currently on treatment with Denosumab at the same schedule. We did not report any serious adverse reaction to Denosumab, mostly for the short length of the treatment over the time in our series.

This retrospective case series analysis was approved by the Institutional Ethic Committee.

Histone 3.3 mutation analysis

The thick tissue sections (7-10µm) of formalin-fixed paraffin-embedded (FFPE) blocks were submitted to an overnight digestion with proteinase K at 56°C. DNA was extracted from FFPE tissues with the Qiamp DNA FFPE tissue kit (Qiagen, Hilden, Germany) accordingly to the manufacturer's protocol in a final volume of 60µL. Nucleic acid samples were checked for concentration and quality by using the NanoDrop ND-1000 Spectrophotometer (Thermo Scientific, Inc., NYSE:TMO).

The primer sets were selected to cover the hot-spot sites of genes and were as following: *H3F3A* (NC_000001.11) forward primer *5'-tgtttggtagttgcatatggtga-3'* and reverse primer *5'-acaagagagactttgtcccatt-3'*; *H3F3B* (NC_000017.11) forward primer *5'-ttatcttcggggcgtctttc-3'* and reverse primer *5'-gagcaggggaggagtgag-3'*. The targeted sequences were tested to exclude nonspecific amplification of homologous regions by UCSC Genome Browser - BLAT Search (http://www.genome.ucsc.edu/cgi-bin/hgBlat?command=start) and Primer-BLAST (http://www.ncbi.nlm.nih.gov/tools/primer-blast/)].

Amplification of both genes was performed in an ABI 2720 thermal cycler (Applied Biosystems-Life Technologies, Foster City, CA 94404, USA) by starting from two different quantity of DNA (20 ng and 100 ng) in a final volume of 20 µl and using HotStarTaq DNA Polymerase (Qiagen, Milan, Italy) with 500nM of each primers. The thermal protocol entailed an initial denaturation at 95°C for 5 minutes, followed by 40 cycles at 95°C for 20 seconds, 58°C for 30 seconds, and 72°C for 30 seconds, with a final elongation step at 72°C for 10 minutes.

PCR products were purified by using FastGene Gel/PCR Extraction kit (Nippon Genetics Europe GmbH, Düren, Germany). DNA fragments were submitted to the cycle sequencing reaction with BigDye Terminator v1.1 Cycle Sequencing Kit (Applied Biosystems-Life Technologies). The purified sequences, obtained by ZR DNA Sequencing

Clean-up Kit (Zymo Research Corporation, Irvine, CA 92614, U.S.A.), were run on an ABI PRISM 310 Genetic Analyzer instrument (Applied Biosystems, Darmstadt, Germany) and manually analyzed.

Sequence variants were reported according to the nomenclature edited by the Human Genome Variation Society (http://www.hgvs.org/mutnomen/recs-DNA.html) considering the nucleotide 1 as the A of the ATG-translation initiation codon.

Immunohistochemistry

For immunohistochemical staining, paraffin-embeddedFFPE tissue sections (5μm) were deparaffined, hydrated and after endogenous peroxidase inactivation immunostained with BenchMark® Ultra stainer (Ventana,Tucson, AZ, U.S.A.), than revealed with iVIEW DAB detection kit, providing a brown reaction product. Table 2 shows antibody source, dilution and antigen retrieval protocol. After completing the staining process, the slides were removed from the autostainer, counterstained with hematoxylin, dehydrated and mounted with a permanent medium. As negative control, we substituted primary antibody with a Ventana dispenser filled with non-immune serum at the same concentration for each immunohistochemical reaction. As positive control, we used reactive bone and bone fracture specimens.

The results of the immunohistochemical staining were evaluated according to a semiquantitative scale as follows: -=0; + <10%; ++=11-49%; +++>50%, both on baseline and on-study specimens. The Ki67 proliferation index was assessed in areas of greater expression determining the percentage of positive cells in at least 200 cells. Determination of tumoral neoangiogenesis in specimens stained with CD31 was performed according to the method of Weidner et al. [5]. Microvascular density (MVD) was assessed in areas containing the greatest number of vascular profiles (hotspots). The analysis was performed in three high power fields for each section of each tumor and the results expressed by average value.

Statistical analysis

All statistical tests were performed using SPSS software (release 12.0). Wilcoxon Signed Rank Test was used to compare the proliferation index and MVD between baseline and on-study specimens. P values <0.05 were considered significant.

Results

Histone 3.3 mutation analysis

We performed direct sequencing for the presence of *H3F3A* (NM_002107.4) and *H3F3B* (NM_005324.4) variants in coding region between codons 1 and 42, including the hot spot codons (28, 35 and 37),We performed capillary sequencing for the presence of H3F3A and H3F3B variants between codons 29 and 63 on DNA extracted from formalin-fixed paraffin-embeddedFFPE tissue. Mutation analysis was carried out in 11 tumors for which non-decalcified specimens were available, and it was successfully performed in 9 tumors, while in 2 instances the quality of extracted DNA was not sufficient to complete the test. Eight tumors presented a p.Gly35Trp (p.G35W; NP_002098.1) mutation in the *H3F3A* gene, while a p.Gly35Val (p.G35V) was detected in one case (Table 1). No mutation was identified in the *H3F3B* gene. In 2 cases it was possible to perform the analysis in pre- and post-treatment tumor samples, and the same p.Gly35Trp (p.G35W) mutation was detected in both specimens.

Histopathology

Post-treatment tumor samples showed pronounced changes in comparison with pre-treatment samples, which mainly consisted of (i) disappearance of osteoclast-like giant cells, (ii) presence of cellular areas formed by sheets of round to ovoid tumor cells, (iii) cellular areas formed by spindle cells arranged in a storiform pattern with little or no extracellular matrix, (iv) areas characterized by the production of abundant fibrillary

extracellular matrix organized in trabecular structures or with a honeycomb pattern (Figure 1). In resection specimens, these histological patterns were not haphazardly distributed, but showed the tendency toward a “zonal” distribution, with more cellular areas in the tumor central portion, and matrix-rich areas in the periphery (Figure 2). Moreover, at the periphery of the tumor, the tumor osteoid-like matrix seemed to merge with the host bone (Figure 2).

Further histological patterns observed in post-treatment samples included the presence of (i) groups of foamy histiocytes interspersed among tumor spindle cells, (ii) focal areas of coagulative necrosis, (iii) areas of round to oval acellular hyaline matrix, sometimes with a rosette-like appearance. In one case, treatment resulted in complete necrosis of the tumor (Figure 1). One Denosumab-treated soft tissue recurrence of GCTB consisted of a neoplastic population of spindle cells arranged in elongated fascicles, with scant extracellular matrix and presence of few osteoclast-like giant cells.

Immunohistochemistry

The results of the immunohistochemical studies are summarized in Table 3 and illustrated in Figure 3.

Cytoplasmic positivity for RANKL was observed in mononuclear tumor cells in all base-line tumor samples, with a percentage ranging between 5% and 10% in most cases, while in 4 cases the staining was more diffuse. Interestingly positive cells were not uniformly distributed within the tumor population, but tended to group together. RANKL expression did not vary significantly in post-treatment samples, with the exception of three cases that showed reduced expression (from ++ to +), and one case that showed increased expression (from + to ++).

In base-line samples, RANK immunostaining was observed in the cytoplasm and/or membrane of osteoclast-like giant cells and in a fraction of mononuclear cells, ranging between 5 and 10%. In on study samples RANK expression was variable, being absent in

2 cases, present in few cells in 7 cases, or present in most tumor cells in 5 cases. Nuclear immunoreactivity for the osteoblastic marker SATB2 was observed in 12 of 15 pre-treatment tumor samples. Positive cells were mononucleated and tended to group within the neoplastic population. Moreover, SATB2 positivity was associated with focal areas of osteoid matrix production in 6 tumors. In post-treatment samples SATB2 expression was detected in 5 tumors, in association with production of osteoid-like matrix, while cellular areas were always negative. All pre-treatment tumor samples showed diffuse nuclear positivity for RUNX2, whereas in post treatment specimens the expression was unchanged in 10 cases, or reduced to less than 10% of cells in 4 cases.

Evaluation of tumor angiogenesis and proliferative activity

In the present series of GCTB, tumor angiogenesis evaluated as MVD decreased significantly after Denosumab treatment. In baseline tumor samples mean MVD was 45.68±9.88 SD (range 27.67-62.33), while in on-study tumor samples it was 19.69±9.68 SD (range 6.00- 40.80) (p=0.001 Wilcoxon Signed Ranks Test). These results are shown in Figure 4.

The Ki-67 labeling index ranged between 7.43% and 38.09% in baseline GCTB samples (mean 20.23±7.19 SD), while it decreased significantly in post-treatment samples, ranging between 4.34% and 18.92% (9.65±5.19 SD)(p=0.001 Wilcoxon Signed Ranks Test). These results are illustrated in Figure 5.

Discussion

The present study confirms that Denosumab treatment induces deep changes in the morphology of GCTB [6-9]. As in previous reports, we noted total or subtotal disappearance of osteoclast-like giant cells, and a residual tumor population formed mainly of spindle cells without atypia, arranged in fascicles, often with a storiform pattern, resulting in a fibrous-histiocytoma like appearance. Areas of collagen matrix formation,

either with a diffuse or a honeycomb/trabecular appearance, merging with osteoid formation, were also visible. However, the analysis of whole tumor section revealed the these areas were not haphazardly distributed, but they were rather organized according to a “zoning” pattern, with more cellular areas in the tumor center and matrix forming areas at the periphery.

Our series of GCTB was characterized at the molecular level for the presence of histone 3.3 mutations. These molecular alterations have been specifically associated with different bone tumor types, since GCTB presents usually G34W mutation (here reported in accordance with adopted nomenclature as p.Gly35Trp) in *H3F3A*, whereas H3 histone 3.3 M3F family 3B mutations have been detected only in a subset of cartilage tumors, including chondroblastoma and chondrosarcoma [2]. The highly specific association of *H3F3A* mutation with GCTB supports its use as a possible diagnostic marker in histologically ambiguous cases, and to screen giant cell rich lesions of bone before Denosumab treatment. In addition, it has been suggested that this histone 3.3 mutation may be relevant for the development of GCTB by inducing osteoclast recruitment, through the alteration of expression of essential osteoclast signaling pathways, such as RANK ligand or colony stimulating factor 1 [2]. In the present series, we confirm that GCTB presents mainly *H3F3A* mutations in Glycine 34, with no involvement of the *H3F3B* gene. Moreover, we detected the same mutation in pre- and post Ddenosumab treatment samples, supporting the hypothesis that this drug does not eliminate tumor cells, but it mainly acts modifying the microenvironment of the tumor and by inhibiting the recruitment of osteoclast-like giant cells. Accordingly, we observed only minor modifications in the immunophenotype of tumor cells, at least regarding the expression of RANK, RANKL and osteoblastic markers.

Previous *in vivo* and *in vitro* studies have shown that GCTB stromal cells are, at least in part, of osteoblast lineage and express osteoblast and pre-osteoblast molecular

markers [10-14]. In order to assess whether Denosumab treatment induces differentiation of the neoplastic cells of GCTB along the osteoblastic lineage, we examined the expression of RUNX2 and SATB2 in pre and post-treatment tumor specimens. In agreement with previous studies [15, 16], we observed that GCTB stains for both markers, although the staining for SATB2 tended to be less diffuse and presented in small groups of neoplastic cells, often associated with osteoid matrix production, whereas RUNX2 was expressed in most neoplastic cells. While RUNX2 expression remained unchanged after treatment, SATB2 was detected only in a subset of cells in areas of mature bone formation, and was not detected in cellular areas or in association with collagen matrix production. Considering that RUNX2 is highly expressed in the early phases of osteoblast differentiation and it is progressively reduced in the mature osteoblasts [17], while SATB2 is important for bone matrix production and mineralization by mature osteoblasts [18-21], our results indicate that the neoplastic cells of GCTB may indeed have a intrinsically defective osteoblastic phenotype which is not or only partially associated with mature bone matrix production after Denosumab treatment. In agreement with this hypothesis, high levels of RUNX2 expression have been associated with reduced osteocalcin production and the maintenance of an immature osteoblastic phenotype [22-24]. However, the low expression of SATB2 in the post-operative specimens might also be explained considering that the median time on pre-operative treatment in our series is 5.7 months which could be a short time for the acquisition of a mature osteoblastic phenotype with new woven bone formation [6].

In the present study, we observed a significant reduction of proliferative activity after treatment, as indicated by the evaluation of the Ki67 labeling index. Similarly, Brandstetter et al., reported a reduction of Ki67 positive tumor stromal cells, although they did not quantify the results [6]. This effect is likely to be due to a modification of the microenvironment, rather than a direct effect, since in vitro studies have not either

demonstrated a significant inhibitory effect on proliferative activity in GCTB cultures [25], or a permanent modification of their phenotype [26].

Here, we first report that Denosumab treatment has an anti-angiogenic effect in GCTB in vivo, as shown by significantly reduced tumor microvessel density. However, the mechanisms responsible for this anti-angiogenic effect need to be elucidated. Previous studies have shown that vascular endothelial growth factor (VEGF) induces RANK expression by endothelial cells, making them more responsive to RANKL effects [27]. Thus, RANKL pro-angiogenic effect could be modulated by VEGF itself through the induction of RANK overexpression. Moreover, RANKL increases vascular permeability and angiogenenesis through an interaction with endothelial nitric oxide synthase (eNOS) [28], independently from VEGF activity [29].

In conclusion, our study confirms that Denosumab treatment induces deep changes in the morphology and biology of GCTB, but does not eliminate tumor cells, as indicated by the persistence of a population with the same H3 histone H3F3A family 3A subunit mutation. The clinical benefit of this treatment appears to be related, at least in part, to a reduction of the proliferative activity and tumor angiogenesis.

Take Home Messages

- GCTB presents mainly *H3F3A* mutations in Glycine 34, with no involvement of the *H3F3B* gene.
- Denosumab treated giant cell tumors of bone show no significant modification of RANK and RANKL expression, and of the osteoblastic markers SATB2 and RUNX2.
- Denosumab induces significant reduction of the proliferative index and of tumor angiogenesis.

Competing Interest: None declared.

Licence for Publication

The Corresponding Author has the right to grant on behalf of all authors and does grant on behalf of all authors, an exclusive licence (or non exclusive for government employees) on a worldwide basis to the BMJ Publishing Group Ltd to permit this article (if accepted) to be published in JCP and any other BMJPGL products and sublicences such use and exploit all subsidiary rights, as set out in our licence (http://group.bmj.com/products/journals/instructions-for-authors/licence-forms).

References

1. Fletcher CDM, Bridge JA, Hogendoorn PCW, Mertens F. WHO classification of Tumours of Soft Tissue and Bone. Vol. 5. WHO Blue Books. WHO Press, 2013.
2. Behjati S, Tarpey PS, Presneau N, et al. Distinct H3F3A and H3F3B driver mutations define chondroblastoma and giant cell tumor of bone. Nat Genet. 2013;45:1479-82.
3. van der Heijden L, Dijkstra PD, van de Sande MA, et al. The clinical approach toward giant cell tumor of bone. Oncologist. 2014;19:550-61.
4. Thomas D, Henshaw R, Skubitz K, et al. Denosumab in patients with giant-cell tumor of bone: an open-label, phase 2 study. Lancet Oncol. 2010;11:275–80.
5. Weidner N, Semple JP, Welch WR, et al. Tumor angiogenesis and metastasis-correlation in invasive breast carcinoma. N Engl J Med 1991;324:1-8.
6. Branstetter DG, Nelson SD, Manivel JC, et al. Denosumab induces tumor reduction and bone formation in patients with giant-cell tumor of bone. Clin Cancer Res. 2012;18:4415-24.
7. Hakozaki M, Tajino T, Yamada H, et al. Radiological and pathological characteristics of giant cell tumor of bone treated with denosumab. Diagn Pathol. 2014;9:111.
8. Akaike K, Suehara Y, Takagi T, et al. An eggshell-like mineralized recurrent lesion in the popliteal region after treatment of giant cell tumor of the bone with denosumab. Skeletal Radiol. 2014;43:1767-72.
9. Santosh N, Mayerson JL, Iwenofu OH. Pseudosarcomatous Spindle Cell Proliferation With Osteoid Matrix Mimicking Osteosarcoma: A Distinct Histologic Phenotype in Giant Cell Tumor of Bone Following Denosumab Therapy. Appl Immunohistochem Mol Morphol. 2015 Mar 16. [Epub ahead of print]

10. Huang L, Teng XY, Cheng YY, et al. Expression of preosteoblast markers and Cbfa-1 and Osterix gene transcripts in stromal tumour cells of giant cell tumour of bone. Bone 2004;34: 393-401.
11. Murata A, Fujita T, Kawahara N, et al. Osteoblast lineage properties in giant cell tumors of bone. J Orthop Sci 2005;10: 581-588.
12. Ghert M, Simunovic N, Cowan RW, et al. Properties of the stromal cell in giant cell tumor of bone. Clin Orthop Relat Res 2007;459: 8-13.
13. Salerno M, Avnet S, Alberghini M, et al. Histogenetic characterization of giant cell tumor of bone. Clin Orthop Relat Res 2008;466: 2081-2091.
14. Steensma MR, Tyler WK, Shaber AG et al. Targeting the giant cell tumor stromal cell: functional characterization and a novel therapeutic strategy. PloS one 2013;8:e69101.
15. Horvai AE, Roy R, Borys D, et al. Regulators of skeletal development: a cluster analysis of 206 bone tumors reveals diagnostically useful markers. Mod Pathol 2012;25:1452-1461.
16. Conner JR, Hornick JL. SATB2 is a novel marker of osteoblastic differentiation in bone and soft tissue tumours. Histopathology 2013;63:36-49.
17. Komori T. Regulation of osteoblast differentiation by transcription factors. J Cell Biochem 2006;99:1233-1239.
18. Dobreva G, Chahrour M, Dautzenberg M et al. SATB2 is a multifunctional determinant of craniofacial patterning and osteoblast differentiation. Cell 2006;125:971-986.
19. Zhang J, Tu Q, Grosschedl R et al. Roles of SATB2 in osteogenic differentiation and bone regeneration. Tissue Engineering Part A 2011;17:1767-1776.
20. Wei J, Shi Y, Zheng L et al. miR-34s inhibit osteoblast proliferation and differentiation in the mouse by targeting SATB2. J Cell Biol 2012;197:509-521.

21. Hassan MQ, Gordon JA, Beloti MM et al. A network connecting Runx2, SATB2, and the miR-23a 27a 24-2 cluster regulates the osteoblast differentiation program. PNAS 2010;107:19879-19884.

22. Komori T. Regulation of osteoblast differentiation by transcription factors. J Cell Biochem 2006;99:1233-1239.

23. Liu TM, Lee EH. Transcriptional regulatory cascades in runx2-dependent bone development. Tissue Eng Part B Rev. 2012;19:254-263.

24. Liu W, Toyosawa S, Furuichi T et al. Overexpression of Cbfa1 in osteoblasts inhibits osteoblast maturation and causes osteopenia with multiple fractures. The J Cell Biol 2001;155:157-166.

25. Lau CP, Huang L, Wong KC, et al. Comparison of the anti-tumor effects of denosumab and zoledronic acid on the neoplastic stromal cells of giant cell tumor of bone. Connect Tissue Res. 2013;54:439-49.

26. Mak IW, Evaniew N, Popovic S, et al. A translational study of the neoplastic cells of giant cell tumor of bone following neoadjuvant Denosumab. J Bone Joint Surg 2014;96:e127.

27. Min JK, Kim YM, Kim YM, et al. Vascular endothelial growth factor up-regulates expression of receptor activator of NF-kappa B (RANK) in endothelial cells. Concomitant increase of angiogenic responses to RANK ligand. J Biol Chem. 2003;278:39548-57.

28. Min JK, Cho YL, Choi JH et al. Receptor activator of nuclear factor (NF)-κB ligand (RANKL) increases vascular permeability: impaired permeability and angiogenesis in eNOS-deficient mice. Blood 2007;109:1495-1502.

29. Kim YM, Kim YM, Lee YM et al. TNF-related activation-induced cytokine (TRANCE) induces angiogenesis through the activation of Src and phospholipase C (PLC) in human endothelial cells. J Biol Chem 2002;277:6799-6805.

Patient	Sex	Age (y)	Tumor site	Type of Surgery	Local Recurrence	Previous surgery	H3F3A	H3F3B
1	F	30	Distal humerus	Curettage	At 12 months§	No	NA	NA
2	F	65	Proximal tibia	Curettage	No	No	NA	NA
3	M	32	Soft tissue°	Resection	No	Yes	NA	NA
4	F	16	Patella	Curettage	At 7 months§	No	p.G35W	WT
5	F	19	Distal tibia	Curettage	No	No	p.G35W	WT
6	F	21	Hand phalanx	Resection	No	No	p.G35W	WT
7	M	62	Distal radius	Curettage	No	No	p.G35W	WT
8	M	29	Distal femur	Curettage	At 11 months§	No	NP	NP
9	F	40	Sacrum	Curettage	No	No	NP	NP
10	F	27	Proximal fibula	Resection	No	No	p.G35V	WT
11	M	26	Proximal radius	Resection	No	No	p.G35W	WT
12	F	43	Proximal fibula	Resection	No	No	NA	NA
13	F	30	Distal femur	Resection	No	No	p.G35W	WT
14	M	31	Distal femur	Curettage	No	No	p.G35W*	WT
15	M	25	Distal tibia	Curettage	No	No	p.G35W*	WT

Table 1. Summary of the clinical features of the series and mutation analysis. M: Male; F: Female. °Soft tissue recurrence of a giant cell tumor of the distal femur treated with curettage 16 months before. § After surgery. NA: specimen not available for molecular analysis due to decalcification; NP: not performed for poor quality DNA. *In these patients both the pre and post-treatment tumor were analyzed and showed the same mutation.

Antibody	Clone and Provider	Species and Dilution	Antigen Retrieval
RANKL	Polyclonal, Abcam, Cambridge, UK	Rabbit, 1:2000	Citrate buffer, ph 6
RANK	64C1385, Abcam, Cambridge, UK	Mouse, 1:200	Citrate buffer, ph 6
SATB2	SATB A4B10, Abcam, Cambridge, UK	Mouse, 1:200	Citrate buffer, ph 6
RUNX2	1D8, Abcam, Cambridge, UK	Mouse, 1:100	Citrate buffer, ph 6
MIB-1	MIB-1, Dako, Glostrup, Danemark	Mouse, 1:40	Cell Conditioning 1, Ventana, Tucson, AZ
CD31	JC70, Cell Marque, Rocklin, CA	Mouse, prediluted	Cell Conditioning 1, Ventana, Tucson, AZ

Table 2. List of the antibodies used in the present study.

Case	RANKL		RANK		SATB2		RUNX2	
	Pre	Post	Pre	Post	Pre	Post	Pre	Post
1	+	+	+	+++	-	-	+++	+++
2	+	+	+	-	+	-	+++	+++
3	+	++	+	+	-	-	+++	+++
4	+	+	+	+++	+	++	+++	+
5	++	+	+	+++	++	-	+++	+++
6	+	NE	+	NE	+	NE	+++	NE
7	++	++	+	-	+	-	+++	+
8	+	+	+	+	-	+	+++	+
9	+	+	+	+	++	++	+++	+++
10	++	+	+	+++	+	-	+++	+++
11	+	+	+	+	+	-	+++	+++
12	+	+	+	+	++	-	+++	+++
13	+	+	+	+	+	+	+++	+
14	++	+	+	+++	+	-	+++	+++
15	+	+	+	+	+	+	+++	+++

Table 3. Summary of the results of the immunohistochemical studies conducted on 15 giant cell tumors of bone treated with Denosumab. Legend: - =0; +<10%; ++ 11-49%; +++>50%; NE: Not evaluated due to diffuse coagulative necrosis.

Figure Legends

Figure 1. Histological appearance of Denosumab treated giant cell tumor of bone. The residual tumor is composed of bland-appearing spindle cells organized in short fascicles with a storiform pattern (A), associated with collagen matrix production. This matrix appears either as thin bands (B), or as thicker connected trabecular structures with a honeycomb appearance (C). Densely collagenized areas, almost devoid of tumor cells, are also seen (D). One tumor was completely necrotic (E).

Figure 2. Giant cell tumor of the proximal fibula after Denosumab treatment. Whole tumor section (left) with corresponding enlarged details (right). The tumor center is almost devoid of cells (A), while moving towards the periphery cellular areas with benign fibrous histiocytoma-like appearance are recognized (B), together with increasing amounts of matrix formation, which progressively assumes the appearance of osteoid matrix (C) and merges with the host cortical bone (D).

Figure 3. Representative images of the immunohistochemical studies. Images on the left column are from baseline specimens, while those on the right column are from on-study specimens. RANK is expressed by a subpopulation of mononuclear cells (A, B), while RANKL is expressed by both multinucleated giant cells and mononuclear cells (C, D). Mononucleated cells show nuclear immunostaining for the osteoblastic marker SATB2 (E), while this marker is not expressed by residual cells after treatment in areas with no matrix formation or with collagen matric production (F). RUNX2 was extensively positive in both pre and post-treatment lesions (G, H).

Figure 4. Denosumab treatment induced a significant reduction of microvessel density (MVD) in the present series of giant cell tumor of bone (p =0.001, Wilcoxon Signed Ranks Test).

Figure 5. Proliferative activity determined as Ki67 labeling index was significantly lower in post treatment specimens (p=0.001, Wilcoxon Signed Ranks Test).

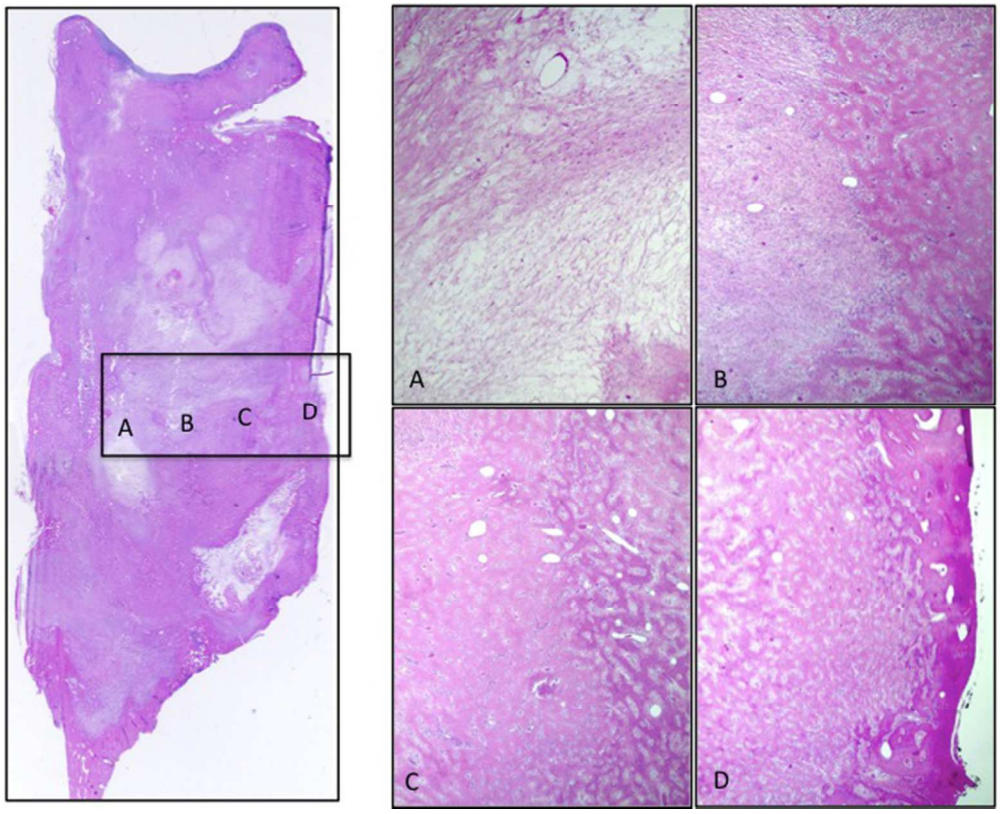

236x189mm (72 x 72 DPI)

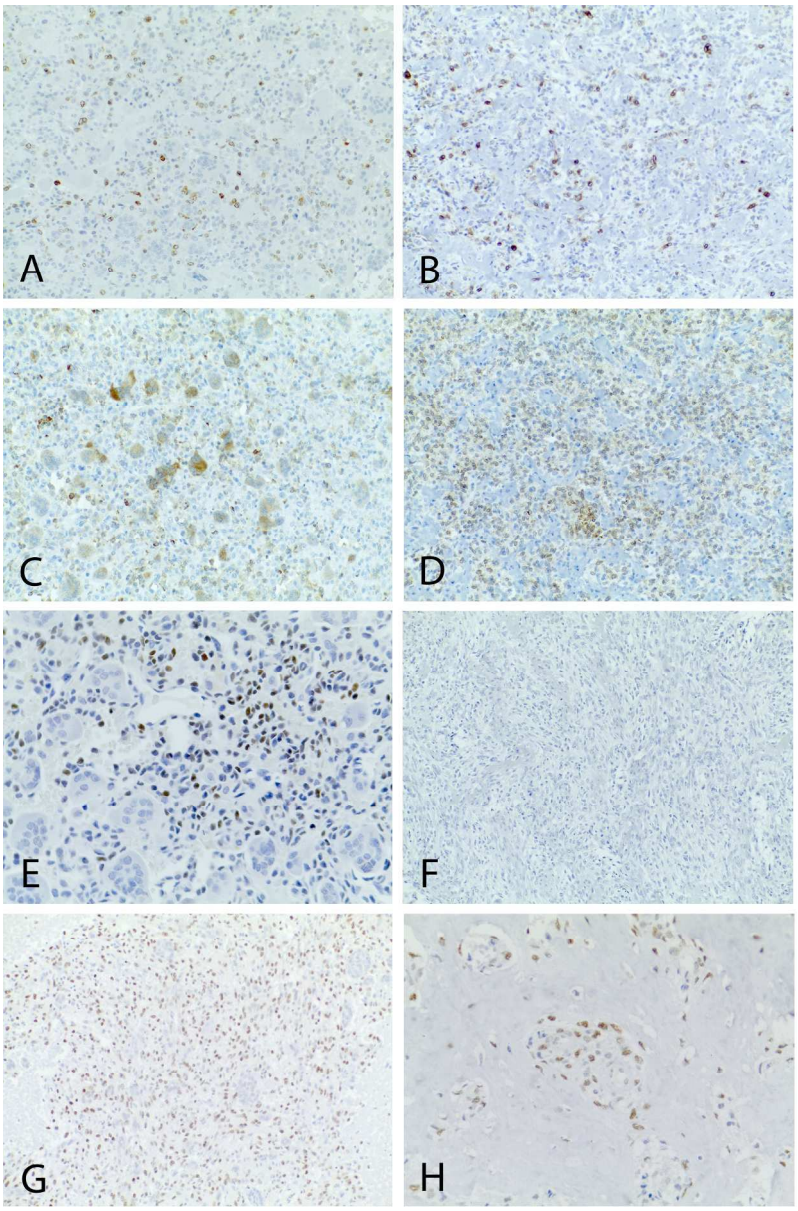

162x245mm (300 x 300 DPI)

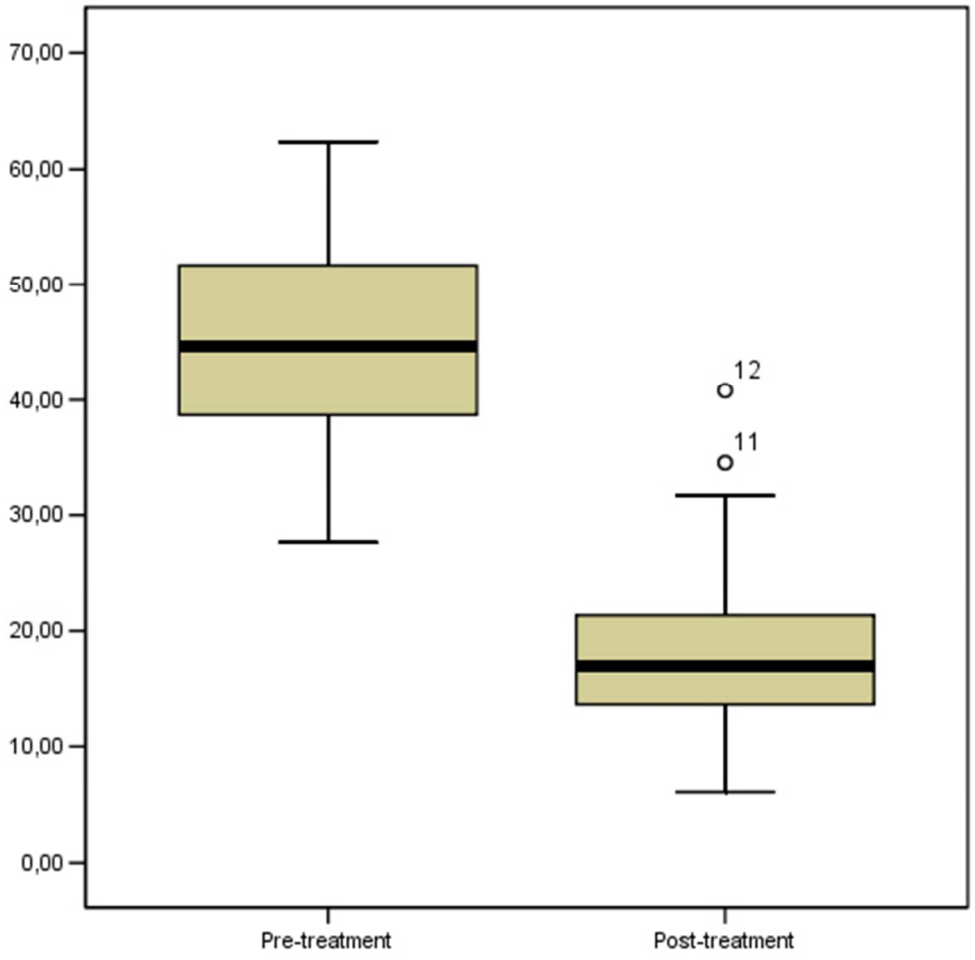

132x132mm (96 x 96 DPI)